

# Resonant Production of Sbottom via RPV Couplings at the LHeC

S. Kaday\*

*Institute of Accelerator Technologies,  
Ankara University, Ankara, Turkey†*

## Abstract

Resonant production of scalar bottom, which is allowed in R-parity violating interactions of supersymmetry, has been investigated at the LHeC collider. Although searching for the physics beyond the standard model is a primary task of the LHC program, recently, an  $e^-p$  collider (LHeC) is proposed to complement and resolve the observation of new phenomena at the TeV scale. In this paper, we have studied on the prospects of improving constraints for  $\hat{L}\hat{Q}\hat{D}$  couplings  $\lambda'_{ijk}$  through the process  $e^- + p \rightarrow \widetilde{b}^* \rightarrow \mu^- + \bar{q}$  where  $q$  denotes the up type quarks. It is shown that constraints on  $\lambda'_{ijk}$  can be improved up to  $10^{-3}$  for  $1\text{ fb}^{-1}$  integrated luminosity at 95% C.L. with 60 GeV  $e^-$  beam option of the LHeC.

arXiv:1304.2124v5 [hep-ph] 11 Jul 2014

---

\*Electronic address: [kuday@science.ankara.edu.tr](mailto:kuday@science.ankara.edu.tr), [kuday@cern.ch](mailto:kuday@cern.ch)

†Electronic address: <http://hte.ankara.edu.tr>

## I. INTRODUCTION

Theoretical structure of supersymmetry (SUSY), which is recently an active area of research and interest at the LHC, allows gauge-invariant and renormalizable interactions that violate the conservation of lepton and baryon numbers. In the framework of minimal supersymmetric standard model (MSSM), these interactions are forbidden by imposing an additional global symmetry that leads to the conservation of a multiplicative quantum number: R-parity [1], which is defined as  $R = (-1)^{3(B-L)+2S}$ , where  $B$ ,  $L$  and  $S$  are the baryon number, lepton number and spin, respectively. As a natural consequence of this phenomenology, all the SM particles and Higgs boson have even R-parity ( $R = +1$ ), while all the sfermions, gauginos and higgsinos have odd R-parity ( $R = -1$ ). One of the highest motivations for R-parity conserved MSSM is that it provides sparticles to be produced in pairs since two odd particles always give even number of R-parity. Although no SUSY signal has been detected yet, pair production of sparticles may be an important clue for final states in SUSY searches at the LHC.

From the theoretical grounds of SUSY, one could expose that R-parity conservation is actually inherited from the conservation of  $B$  and  $L$  quantum numbers which is the natural consequences of a renormalizable and a Lorentz invariant theory. For such an extended SM theory, it is not necessary to keep those variables still conserved as long as the algebraic structure is safe. Although non-conservation of both  $B$  and  $L$  quantum numbers leads to rapid proton decay, a firm restriction to RPV (R-Parity Violating) couplings guarantees a stable proton. Furthermore, allowing many of the interactions with the sparticles in the RPV SUSY model provides even richer phenomenology comparing to the other models. However, many of the interactions in these terms may appear to be strictly suppressed in the nature. Thus, practical application of RPV in MSSM also reveals several implications: firstly, sparticles can be produced in resonance processes as well as in pairs and secondly stabilization of particles (e.g.: dark matter) may not be guaranteed directly. It has been showed that in the context of bilinear RPV model both gravitino [2, 3] or axino [4] as dark matter are consistent with a lifetime exceeding the age of universe. Considering the neutrino issue in the SM, bilinear RPV which is induced by bilinear terms in the superpotential can explain the neutrino masses and mixings in compatible with the current data without invoking any GUT-scale physics [5].

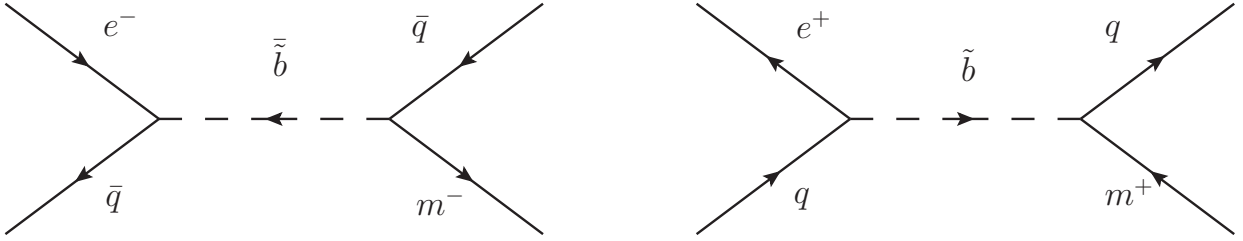


Figure 1: Feynman diagrams of signal production where  $q = u, c$  quarks

From the recent experimental data, the highest constraints for gluino mass reached about 1.5 TeV with 95% C.L. in GMSB and CMSSM searches at  $\sqrt{s} = 8 \text{ TeV}$  according to the ATLAS [6] and CMS [7] results. For stop and sbottom masses, recent constraints are  $m(\tilde{t}) > 660 \text{ GeV}$  [8] for  $L = 20.5 \text{ fb}^{-1}$  and  $m(\tilde{b}) > 620 \text{ GeV}$  [9] for  $L = 12.8 \text{ fb}^{-1}$  at the LHC. Ongoing researches that can be interpreted in the context of R-parity violating supersymmetric scenarios at the LHC set the limit  $\tilde{q} > 700 \text{ GeV}$  [10, 11] for squark masses in muon + jets final states.

As the continuation of the LHC physics program, LHeC [12, 13] can extend these researches into the unexplored high mass regions with a linac-ring configuration which has been decided in the CDR [14] to continue technical design work. It should be emphasized that the parameter space which will be covered at the LHeC, also intersects with LHC searches, so that the main motivation of this work will be to compare limits between the LHeC as the future collider and LHC as the recent collider and to search for a possibility to improve those limits. After the LHeC starts running in full power, the first task will be to reconsider those limits and improve them to constraint R-parity violating squarks. Throughout this work, we will consider the basic energy option as the main reference for LHeC, namely,  $e^\pm = 60 \text{ GeV}$  and  $p = 7 \text{ TeV}$  with  $L = 10^{33} \text{ cm}^{-2}\text{s}^{-1}$ .

## II. SIGNAL PRODUCTION AND DECAY VIA RPV INTERACTIONS

The R-parity violating extension of the MSSM superpotential is given by

$$W_{RPV} = \frac{1}{2}\lambda_{ijk}\epsilon^{ab}L_i^aL_j^b\bar{E}_k + \lambda'_{ijk}\epsilon^{ab}L_i^aQ_j^b\bar{D}_k + \frac{1}{2}\lambda''_{ijk}\epsilon^{\alpha\beta\gamma}\bar{U}_i^\alpha\bar{D}_j^\beta\bar{D}_k^\gamma \quad (1)$$

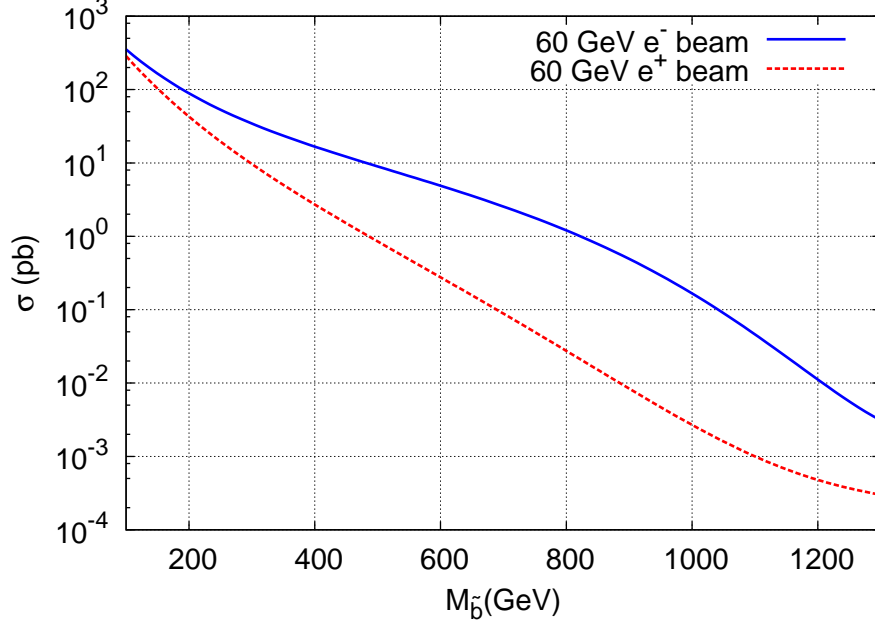


Figure 2: Cross sections vs. sbottom mass

where  $i, j, k = 1, 2, 3, 4$  are the family indices;  $a, b = 1, 2$  are the  $SU(2)_L$  indices and  $\alpha, \beta, \gamma$  are the  $SU(3)_C$  indices.  $L_i(Q_i)$  are lepton (quark)  $SU(2)$  doublet superfields;  $E_i(D_i, U_i)$  are the charged lepton (down-type and up-type quark)  $SU(2)$  singlet superfields. The couplings  $\lambda_{ijk}$  and  $\lambda''_{ijk}$  correspond to the lepton number violating and baryon number violating couplings, respectively. One can easily see that the  $\lambda'_{ijk}$  coupling constants are antisymmetric under the exchange of the first two indices and extract the  $\lambda'_{ijk}$  part of the Lagrangian as;

$$L_{\lambda'} = -\lambda'_{ijk} [d_{Rk}^\dagger \bar{\nu}_i^c P_L d_j + \tilde{d}_{Lj} \bar{d}_k P_L \nu_i + \tilde{\nu}_i d_k P_L d_j - d_{Rk}^\dagger \bar{e}_i^c P_L u_j - \tilde{e}_{Li} \bar{d}_k P_L u_j - \tilde{u}_{Lj} \bar{d}_k P_L e_i] + h.c. \quad (2)$$

Here, the fourth term directly corresponds to the vertex factors of the diagrams in Fig.1. So one can write the parton-level differential cross section for signal in the rest frame of final muon and quark states as;

$$\frac{d\sigma}{d\Omega} = \frac{(\lambda'_{123} \lambda'_{232})^2}{(16\pi)^2} \frac{\hat{s}}{(\hat{s} - m_{\tilde{b}}^2)^2 - (\Gamma m_{\tilde{b}})^2} \quad (3)$$

where  $m_{\tilde{b}}$  is sbottom mass and  $\Gamma$  is the total width of sbottom that can be calculated as  $(\lambda'_{ijk})^2 m_{\tilde{b}} / 8\pi$ .

Since we take the single dominance hypothesis for granted, lighter sbottom mass eigen-

state will be the actual object here whenever we refer to sbottom. For the signal production, one could immediately calculate that the contributions of other down type scalar superpartners are negligible and parton-level contributions of all other quarks are minor except  $u, c$  quarks. Therefore, we have taken into account these contributions to evaluate the total cross sections as in Fig.2 using the COMPHEP [15] event generator and CTEQ6M PDF [16] package. In SUSY phenomenology, the magnitudes of the RPV couplings are arbitrary, and they are restricted only from the phenomenological considerations. Therefore two standard bounds are taken as [17];

$$\lambda'_{113} = \lambda'_{123} \leq 0.18, \quad \lambda'_{231} = \lambda'_{232} \leq 0.45 \quad (4)$$

Here, it is worthwhile to emphasize that for electron and positron beam options, calculations explicitly show that the  $e^-$  beam options always deliver the highest cross section values, even for 60 GeV  $e^-$  beam option in the low mass region. This result seems to be contrary with the stop resonance production at the LHeC [18] where  $e^+$  beam option delivers the higher cross section values. The main reason of that difference is related with the subprocess  $e^- + q \rightarrow \widetilde{b}^* \rightarrow \mu^- + \bar{q}$  where  $q$  denotes  $u, c$  quarks whereas for stop production main contribution comes from  $b$  quarks in the initial state. Therefore, equation [3] yields to stronger signal values than that of the stop resonance production. For the rest of this work, we choose 60 GeV  $e^-$  beam option as the default option for investigating kinematical distributions and exclusion limits.

### III. BACKGROUND PROCESSES

The process  $e^\pm + p \rightarrow \mu^\pm + q/\bar{q} + X$  where  $q$  denotes  $u, c$  quarks seems to be the main background resource for both beam options at the LHeC. The reducible SM background comes through the subprocess  $e^- + p \rightarrow \nu_e + q/\bar{q} + W^-$  where W boson rapidly decays via  $\mu^- \bar{\nu}_\mu$  channel. Note that, vetoing  $b/\bar{b}$  quark contributions in the final state reduces these subprocesses for considerable amount. In experimental point of view, the background may even be reduced more if c-tagging option implemented for the final state quarks. In our case, we didn't take into account any c-tagging options because of the considerably low tagging efficiencies. We have obtained the comparisons of kinematic distributions for backgrounds and for RPV signals using PYTHIA 6.4 [19] and COMPHEP [15] respectively as in Fig.3

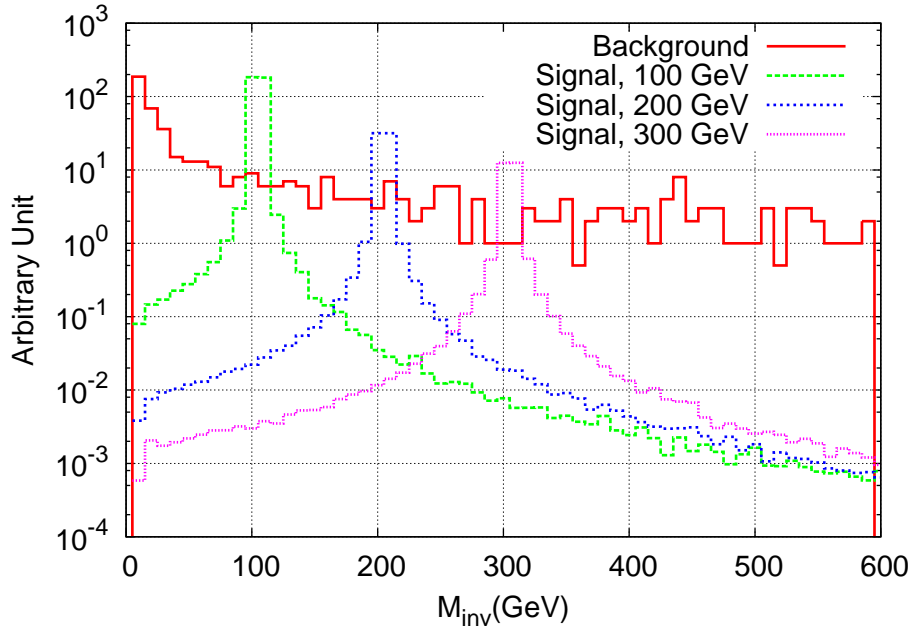


Figure 3: Invariant mass distribution of signal and background

and Fig.4. We have built a new model implementing RPV interactions and vertex factors in COMPHEP for signal while we have used SM event generator of PYTHIA 6.4 [19] for background normalizing over  $10^4$  events.  $P_T$  distributions of the jets in the final states will be naturally at the order of half sbottom mass since outgoing particles, muon and jets are back-to-back in the transverse plane neglecting the missing transverse energy. Since we have neutrinos that will escape from detection in the final states leaving a significant missing transverse energy, it is important to have non-zero  $\cancel{E}_T$  distribution as in Fig.5.

#### IV. EVENT SELECTION AND DISCUSSION

For event selection part of the analysis, a strict strategy has been introduced before for RPV resonance particles [18] in order to reduce large SM background. In our case, we have developed the following cuts and optimizations:

- Kinematic cuts: for muons  $p_T^\mu > 25$  GeV and  $|\eta_\mu| < 2.5$ ; for jets  $p_T^q > 25$  GeV and  $|\eta_q| < 3.5$ .
- Missing transverse energy veto:  $\cancel{E}_T < 25$  GeV.

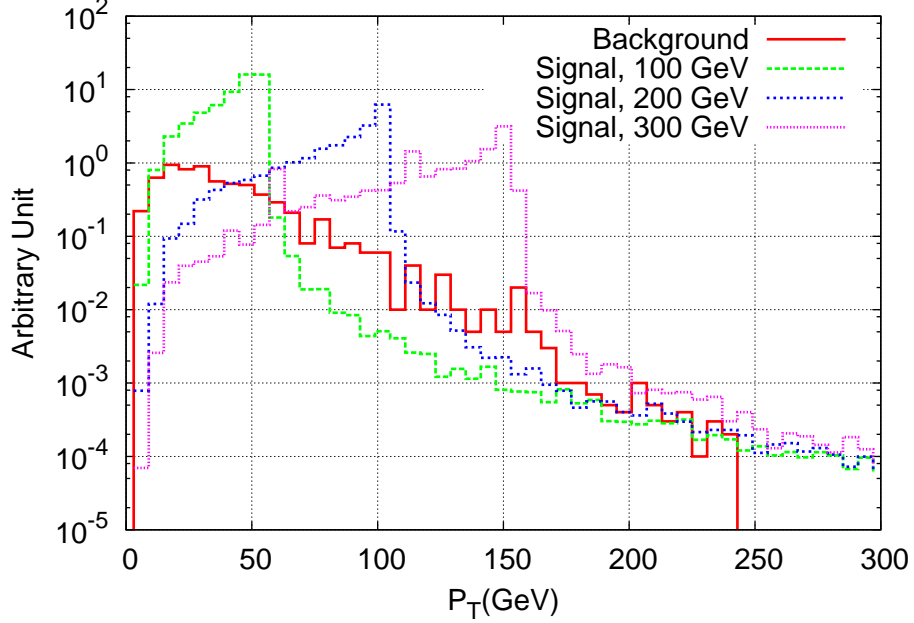


Figure 4: Transverse momentum for jets

- Invariant mass cut:  $M_{\mu q} > 85$  GeV and mass window cut in accordance with the energy resolution.
- Vetoing b-jets with 60% efficiency: Same assumption for b-jet identification in experiments since we need to identify b-jets before vetoing.

After implementing above selection criteria, background cross sections are calculated as 1.7 fb for 60 GeV  $e^-$  beam option and 1.6 fb for 60 GeV  $e^+$  beam option. For signal production, events always survived not below than 85% for sbottom masses between 100 and 1000 GeV. In Table.I, one can see the required luminosities to reach  $2\sigma$  significance value (95% C.L.) for both 60 GeV  $e^-$  beam and 60 GeV  $e^+$  beam options. In significance calculations, we have always used  $S/\sqrt{S+B}$  formulation where  $S$  number of signal and  $B$  number of background events. It is obvious that LHeC can exclude sbottom mass up to 1000 GeV in its first runs with  $217.5 pb^{-1}$  integrated luminosity if there is no apparent excess from SM predictions on  $\mu + jets$  final states. Likewise, we depicted an extended plot of Table I in Fig.6. Attainable limits for sbottom mass with respect to RPV couplings  $\lambda'_{113} = \lambda'_{123}$  and  $\lambda'_{231} = \lambda'_{232}$  are presented in Fig.7 at 60 GeV  $e^-$  beam option of LHeC for  $1 fb^{-1}$  integrated luminosity. One can see here that LHeC can exclude sbottom mass up to 1200 GeV. The main reason of

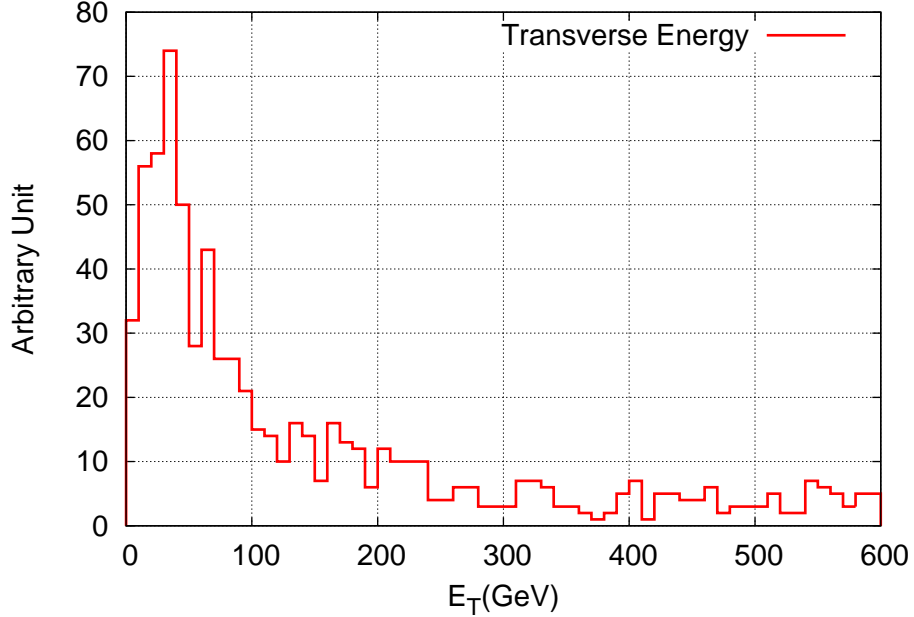


Figure 5: Missing transverse energy of the total background

$\lambda'_{113} = 0.18$  line extending to high mass region is a few survived backgrounds events after selection criteria. With respect to the recent limits of sbottom mass ( $\sim 700$  GeV), minimum attainable limits to RPV couplings  $\lambda'_{232}$  calculated at around 0.25 for a fixed  $\lambda'_{113} = 0.18$  value.

## V. CONCLUSION

In this study, we introduced a phenomenological approach for constraining  $\hat{L}\hat{Q}\hat{D}$  couplings via RPV  $e^- + p \rightarrow \widetilde{b}^* \rightarrow \mu^- + \bar{q}$  process ( $q = u, c$ ). Resonance production of sparticles via RPV processes is a great advantage for obtaining a stronger signal although the specific final states can broaden the total background just as in our case for  $\mu + \text{jets}$  final state. We implemented a stricter event selection in the limits of experimental capabilities to optimize the sensitivity of signal. Considering 60 GeV  $e^\pm$  beam options of LHeC, we presented the cross sections and required luminosities at 95% C. L. for  $\lambda'_{113} = \lambda'_{123} = 0.18$  and  $\lambda'_{231} = \lambda'_{232} = 0.45$  and attainable limits for sbottom mass with respect to RPV couplings. In conclusion, LHeC can extend the exclusion limits of  $\hat{L}\hat{Q}\hat{D}$  couplings up to  $10^{-3}$  for  $1 \text{ fb}^{-1}$  integrated luminosity at 95% C.L. with 60 GeV  $e^-$  beam option.

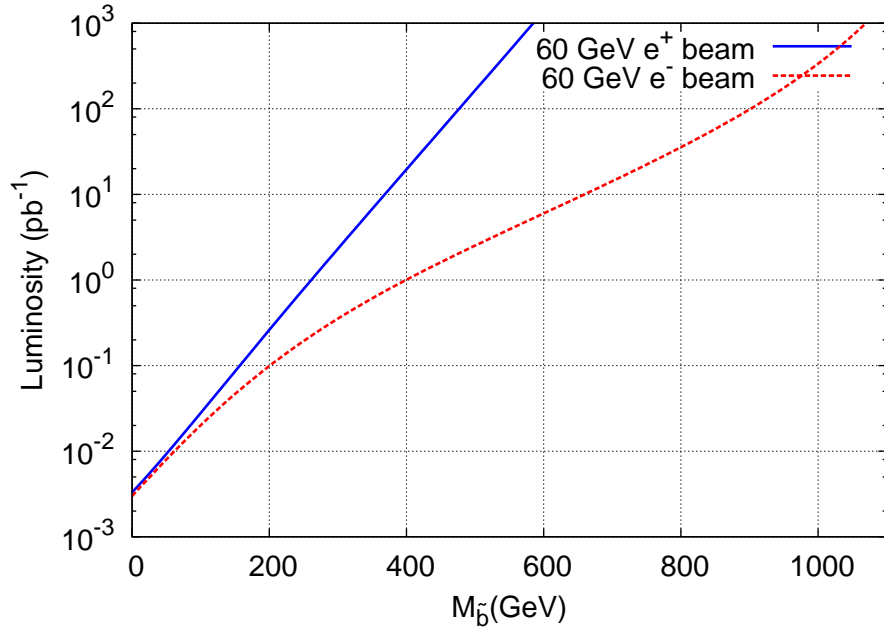


Figure 6: Integrated luminosity vs. sbottom mass for 95% C. L.

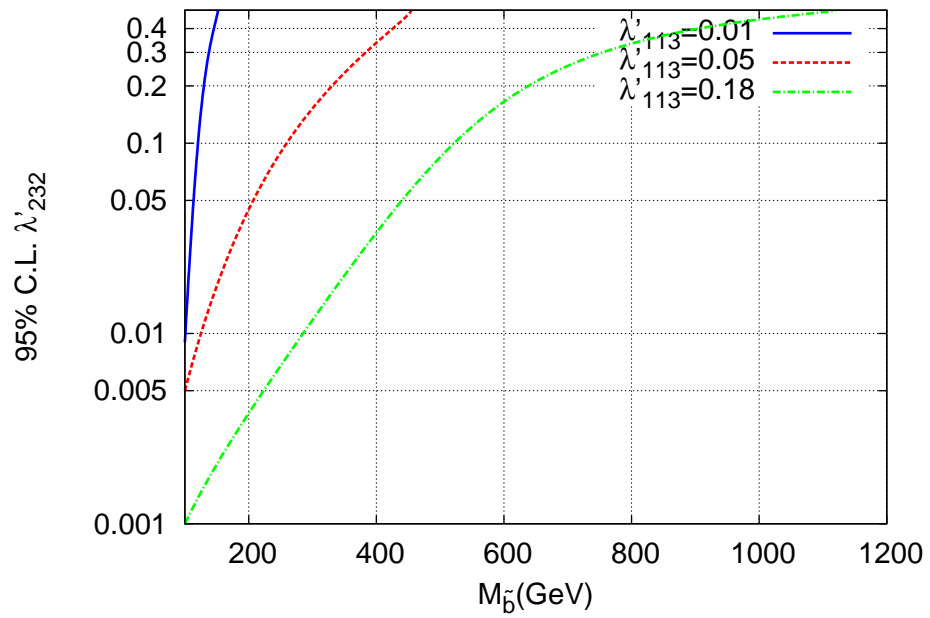


Figure 7: Attainable limits for the sbottom mass and RPV couplings at 60 GeV  $e^-$  beam option of LHeC

$M_{\tilde{b}}$ (GeV)	$\sigma(e^-p)$ (pb)	Required $L_{int}(e^-p)(pb^{-1})$	$\sigma(e^+p)$ (pb)	Required $L_{int}(e^+p)(pb^{-1})$
100	211.78	0.022	201.38	0.023
200	38.39	0.154	22.17	0.318
300	13.71	0.492	4.85	2.5
400	6.82	1.192	1.35	18.836
500	3.76	2.683	0.41	157.761
600	2.1	5.707	0.13	$1.382 \times 10^3$
700	1.11	13.547	$3.78 \times 10^{-2}$	$1.321 \times 10^4$
800	0.53	32.010	$1.3 \times 10^{-2}$	$7.3 \times 10^4$
900	0.21	79.491	$2.1 \times 10^{-3}$	$11.738 \times 10^5$
1000	$6.55 \times 10^{-2}$	217.423	$3 \times 10^{-4}$	$14.37 \times 10^6$

Table I: Required luminosities and cross sections of sbottom at the 60 GeV  $e^\pm$  beam option of LHeC for 95% C.L. with  $\lambda'_{113} = \lambda'_{123} = 0.18$  and  $\lambda'_{231} = \lambda'_{232} = 0.45$

### Acknowledgments

I would like to express my greatest gratitude to Saleh Sultansoy for his fruitful discussions and helpful comments. This work is partially supported by Turkish Accelerator Center (TAC) Project, Turkish Atomic Energy Authority (TAEK) and T.R. Ministry of Development (DPT).

- 
- [1] R. Barbier, C. Berat, M. Besancon, M. Chemtob, A. Deandrea, E. Dudas, P. Fayet, S. Lavignac, G. Moreau, E. Perez, and Y. Sirois, Phys. Rept. 420, 1 (2005).
  - [2] M. Fukugita and T. Yanagida, Phys. Lett. B 174 (1986) 45, arXiv: 0005214 [hep-ph].
  - [3] M. Hirsch, W. Porod and D. Restrepo, JHEP 0503, 062 (2005) arXiv:0503059 [hep-ph].
  - [4] E. J. Chun and H. B. Kim, JHEP 0610 (2006) 082, arXiv:0607076 [hep-ph].
  - [5] W. Buchmuller, L. Covi, K. Hamaguchi, A. Ibarra and T. Yanagida, JHEP 0703, 037 (2007), arXiv: 0702184 [hep-ph].
  - [6] G.Aad *et al.*, (ATLAS Collaboration), arXiv:1210.1314 [hep-ex].
  - [7] S.Chatrchyan *et al.*, (CMS Collaboration), arXiv:1303.2985 [hep-ex].

- [8] ATLAS Collaboration, Report No: [ATLAS-CONF-2013-024].
- [9] ATLAS Collaboration, Report No: [ATLAS-CONF-2012-165].
- [10] G.Aad *et al.*, (ATLAS Collaboration), arXiv:1210.7451 [hep-ex].
- [11] CMS Collaboration, Report No: [CMS PAS SUS-13-003].
- [12] The LHeC web page, <http://www.lhec.org.uk>.
- [13] CERN-ECFA-NuPECC Workshop on the LHeC, Chavannes, Switzerland, June 2012, see <http://cern.ch/lhec>.
- [14] J. L. Abelleira Fernandez et al. [LHeC Study Group Collaboration], *J. Phys. G* 39, 075001(2012); arXiv:1206.2913 [physics.acc-ph].
- [15] E. Boos, V. Bunichev, M. Dubinin, L. Dudko, V. Edneral, V. Ilyin, A. Kryukov, V. Savrin, A. Semenov, and A. Sherstnev, *Nucl. Instrum. Meth. A* 534 250 (2004).
- [16] J. Pumplin, D. R. Stump, J. Huston, H. L. Lai, P. Nadolsky, and W. K. Tung, *JHEP* 0207.012 (2002).
- [17] R. Barbier, C. B´erat, M. Besancon, M. Chemtob, A. Deandrea, E. Dudas, P. Fayet, S. Lavignac, G. Moreau, E. Perez, and Y. Sirois, *Phys. Rept.* 420, 1 (2005).
- [18] W.Hong-Tang, Z. Ren-You, G. Lei, H. Liang, M. Wen-Gan, L. Xiao-Peng and W. Ting-Ting, arXiv:1107.4461 [hep-ph], *JHEP* 1107.003 (2011).
- [19] T. Sjostrand, S.Mrenna, P. Skands, “PYTHIA 6.4 Physics and Manual”, *JHEP* 0605.026 (2006).